Hexahedron Reverberation Box for Measurement of Frequency Dependent Reverberant Noise Absorption Coefficient and Experimental Verification

Mallika DATTA
Government College of Engineering and Textile Technology, Serampore, 12, William Carey Road, Hooghly-712201, West Bengal, India, dattamallika8@gmail.com

Gautam BASU
ICAR-National Institute of Natural Fibre Engineering and Technology, 12, Regent Park, Kolkata 700040, India, gbose91@gmail.com

Devarun NATH
Government College of Engineering and Textile Technology, Serampore, 12, William Carey Road, Hooghly-712201, West Bengal, India, ndevarun@icloud.com

Kartick K. SAMANTA
ICAR-National Institute of Natural Fibre Engineering and Technology, 12, Regent Park, Kolkata 700040, India, karticksamanta15@gmail.com

Surajit SENGUPTA
ICAR-National Institute of Natural Fibre Engineering and Technology, 12, Regent Park, Kolkata 700040, India, ssg_42@rediffmail.com

Sayandeep DEBNATH
ICAR-National Institute of Natural Fibre Engineering and Technology, 12, Regent Park, Kolkata 700040, India, sayandeepdebnath@yahoo.in

Abstract: - A hexahedron reverberation box has been developed through reverse engineering to study the reverberation time of fibrous felts in diffuse acoustic field condition. The study reinstated the frequency as a prime factor to understand the relation between noise control performance of a sample in transfer matrix method and diffused acoustic field condition. A new non-linear, bi-variant frequency dependent model was formulated through synchronization of impedance tube data and noise absorption coefficient calculated from reverberation time of the felts tested in the hexahedron box. The empirical model was validated for particle board based perforated absorber which yielded a comparable noise absorption value with a mean absolute error as low as 0.02. The reverberation box substantially reduces the size of samples for trial in nondestructive mode. The frequency dependent model for different absorber predicted the noise absorption property from calculated reverberation time (RT60), which would help in engineering specified samples for noise control. The novelty of the work lies in the fabrication of the reverberation box to work with frequency levels as low as 250 Hz i.e., above Schroeder frequency.

Keywords: Diffused acoustic field; hexahedron reverberation box; noise absorption coefficient; reverberation time; Schroeder frequency.

1. INTRODUCTION

The primary acoustic elements engaged in the control of noise are sound absorbers, reflective surfaces, and diffusers. The use of reflective surfaces and diffusers preserve and dispense the sound energy, while the sound absorber reduces the sound levels and controls reverberation. Reverberation, in acoustics, is one of the major parameters, which need to be measured for designing noise free architectural engineering of an auditorium or workplace [1]. A reverberation is created when sound waves/signals are reflected from the barrier(s) at the vicinity, causing a large number of coherent reflective waves and then decay as the sound energy is absorbed by the surfaces of objects in the space [2]. However, for the satisfaction of the listener of a musical node or a speech, a certain extent of reverberation is desirable to embellish the direct sound and adds qualities of fullness, warmth, and cohesion to the musical piece. Due to the important effect of reverberation on listening perception, reverberation time has become an important parameter in acoustic for designing of the venue as well as insulation system [3]. Reverberation time is the time, in second that would be required for the sound pressure level to decrease by 60 dB after the sound source is stopped, commonly called 'RT60'[4]. It is reported that the optimal reverberation time for a sound cloud environment ranges from 0.4 s to 0.5 s [5].

The concept of reverberation was introduced by Sabine [6]. Sound absorption characteristic in the diffused acoustic field is measured in the reverberation room following the international standard procedure ISO 354-2003 which requires minimum space, 294 m^3 inside the reverberation room [7]. The requirement of samples at the present standard method is very large, even up to 12 m^2.

Estimation of reverberation time in a room of different shapes and with varying absorber positions to fit in the Sabine model were reported [8], [9]. But, the researchers concluded that Sabine's model missed out on some major parameters viz., the shape of the room and relative position of the absorber, method of sample mounting, and especially, frequency of sound which, could influence the estimated noise absorption by the reverberation room. Some methods have also been suggested to measure the diffuseness of the reverberation room [10]–[12].

Robin et al. [13] estimated absorption coefficients using a synthesized diffused acoustic field of excitation, which were in good agreement with those obtained from the transfer matrix method/impedance tube method with the lowest frequency level of 400 Hz. Few approaches were taken up for modelling and predicting reverberation time in a rectangular room with non-uniform absorption distribution has been reported [14], [15], which did not follow the principle of diffused acoustic field (DAF). However, no work so far is available in the literature on development of small size portable reverberation room to analyze noise control performance at frequency level below 400 Hz under the diffused acoustic field of excitation.

Designing a hexahedron reverberation box with a diffuse acoustic field (DAF) of in-situ condition works in a frequency range starting at 250 Hz (wavelength of 135 cm) is the focus of the current work. The attempt to design a hexahedron box would aids to test samples in a nondestructive manner with smaller size (1m^2), confirmed by using the typical commercial samples (rockwool and glasswool), and finally validated with natural fiber based felts. The work demonstrated a prediction model based on the synchronization of noise absorption coefficient (NAC) values generated by an impedance tube, using the transfer matrix principle and reverberation time, considering frequency as the prime factor. The developed empirical model was validated for a perforated absorber made of particle board.

2. EXPERIMENTAL WORK

2.1. Fabrication of Reverberation Box

The reverberation box (Figure 1) is a vibration free small box designed to create a diffused acoustic field (DAF). The DAF was excited by a continuous broadband pink noise source i.e., a noise generator. When the pink noise generator was suddenly switched off, the reverberation of sound inside the box survived owing to the numerous internal reflections from the surface walls of the box. The time lapse to reduce the sound level by a specific magnitude of 20 and 30 dB was then measured to calculate the reverberation time.

The reverberation box was having a flat floor and four sides (walls) were fixed perpendicularly to the floor. The arrangement of the sidewall was designed in such a way that the opposite walls were not parallel to each other. The four walls of the box touched the angled roof to meet the condition of unequal lengths. The floor formed two right angles at the opposite corners of the box. All the floors and roof were made of glass fiber reinforced composite sheet having a wall thickness of 50 mm. The use of a laminar mold for making the walls of the reverberation box from glass fiber composite provided very smooth surfaces and reduces effect of rough surface [16]. The non-parallel walls (including the roof) were thus designed as reflecting and non-planar shields in random positions to reflect and diffuse the waves in all possible directions to maintain the diffused acoustic field (DAF). The structure of the box was made vibration free and robust to avoid absorption of sound by the wall. The boundaries of all physical enclosures vibrate in response to incident sound and are to some extent sound absorptive [17]. The lower limiting frequency (f_l) calculated from the minimum distance (x) between the opposite walls was greater than the half of maximum wavelength of the sound energy to maintain the DAF and may calculated from the following equation[18].

$$x > \frac{\lambda_{max}}{2} \quad (1a);$$

where λ_{max} is the maximum wavelength. The 250 Hz was set as the lower frequency limit (f_l) of portable reverberation box to calculate the minimum distance between the opposite wall at 65 cm. The upper limit of the frequency was fixed based on the central frequency of ⅓ octave band and frequency domain of the impedance tube based on transfer- function method, ISO 10534-2:1998. The jute felt was tested in the frequency range of 250 to 6000 Hz. The maximum length of the wall (L_{max}) was worked out using the following equation[18].

$$L_{max} \leq 1.9V^{\frac{1}{3}} \qquad (1b);$$

Castors with pedal brakes were attached at the bottom of the machine for its easy portability and to eliminate the chance of vibration during testing[19]. The total weight of the portable box was nearly350 kg and the total floor space required to install the box is 3.15 m^2. A collapsible aperture was provided attached to the front wall of the box, much nearer the floor, for ease of placement/mounting of the sample inside the box. The schematic diagram of the reverberation box is given in Figure 1.

2.2. Determination of Volume of Box

The complex dimension of the box made it difficult to estimate the volume of the portable reverberation box. So, a three-dimensional (3D) drawing of the inner surface of the proposed box was made through SpaceClaim software. Volume of the box was found to be 2.84 m^3 whereas the area of the inner surfaces is 12.36 m^2.

2.3. Accessories of Reverberation Box

Figure (2) shows the various accessories attached to the portable reverberation box. The power supply of 230V and 50 Hz AC had converted into 11.0 V DC for suppling to pink noise generator (Phon-X, Ntek, Italy). The sound source attached to the reverberation box generated pink noise, which is characterized by uniform acoustical energy, distributed over the octave of the audio spectrum of human hearing (20 Hz to 20 kHz) to maintain the condition of the diffused field [20]. An electro-acoustic transducer or loudspeaker was placed at the top corner of the box.

The Pink noise generator with an amplifier was connected in line with the loudspeaker for gradual change in noise level. A voltmeter was used to regulate the amplitude of the signal of the pink generator fed to the speaker. A portable 'sound level meter', SLM (Rion, NL52 RV, Japan) was used for measuring RT20 and RT30. The extended microphone was hanged from the centre of the roof of the box by a tripod and was connected to SLM through 'speakON' four contact twist-lock connecting cable of φ 1.5 mm.

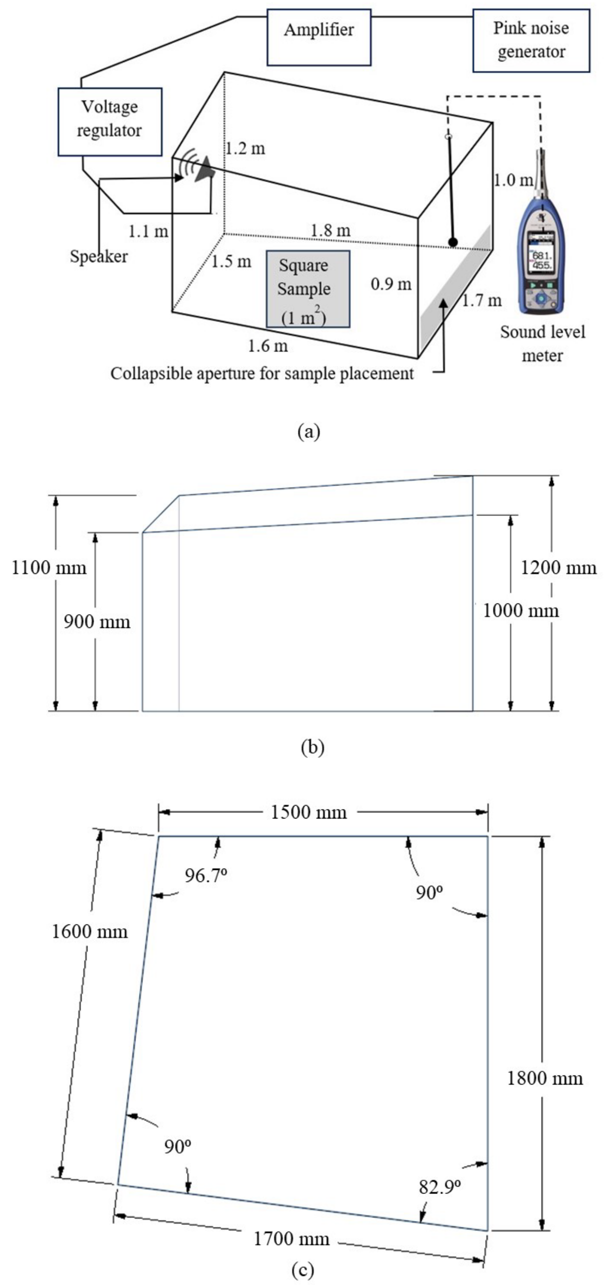

Figure 1. (a) Schematic diagram of the reverberation box. (b) and (c) 3D Engineering drawing through Space Claim.

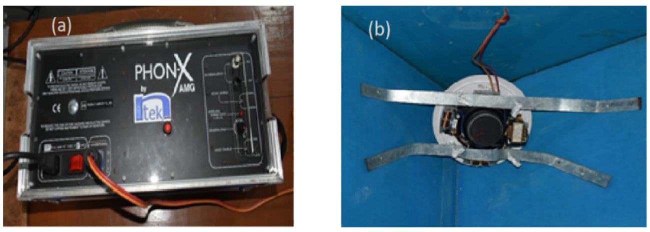

Figure 2. Accessories attached to developed reverberation box: (a) Pink noise generator with amplifier (Make-Phon-X, Italy) and (b) Placement of speaker.

2.4. Calculation For Microphone Position

When the microphone was inserted into the portable reverberation box, it was aligned to the walls of the box and the critical distance (*D*) of the receiver or the microphone from the source are determined as per the volume (*V*) of the box using the following equation [21], [22]:

$$D = 0.057 \times \sqrt{\frac{V}{C \times RT60}} \quad (1c).$$

where, *C* is the speed of the sound, and RT60 represents the reverberation time to decay sound energy by 60 dB after the termination of emission of sound. The microphone connected to the sound level meter was sealed to avoid air leakage to the outside of the box.

2.5. Preparation of Felts

Felts of different fiber (banana, coir, cotton, flax (tow), hemp, jute, okra, sisal) based absorbers of nominal thickness, 15 mm and of 1650 g/m^2 areal density were fabricated using in needle punching loom for making nonwoven (Fehrer, Austria) at a local jute mill (Figure 3). The commercially available absorbers (glass and rockwool, 40 mm thick) were sourced from the market for the study. The raw fibers were sprayed with oil (2%)-in-water emulsion and conditioned in an enclosed chamber for 48 h before processing in a softening machine. The output was then passed through fiber opening machines (1st and subsequently 2nd carding machine) for fiber separation, where fiber streaks were stretch broken to form open fibrous material. The fibrous mass was then passed through the camel back cross lapper and feed to needle punching machine.

The Thickness of felts was measured using a footstep-type thickness tester under a circular foot (φ 20 mm) with a pressure of 8.5 kPa for 60 min following ASTM D1777.

Figure 3. Assembly of different fibers.

2.6. Determination of Reverberation Time Using Hexahedron Reverberation Box

Reverberation time was experimentally measured from decay curves obtained from SLM after placement of one square meter felt on the floor of the box (Figure 4).

Figure 4. The photograph shows the ease of placement of felt samples through a collapsible. aperture.

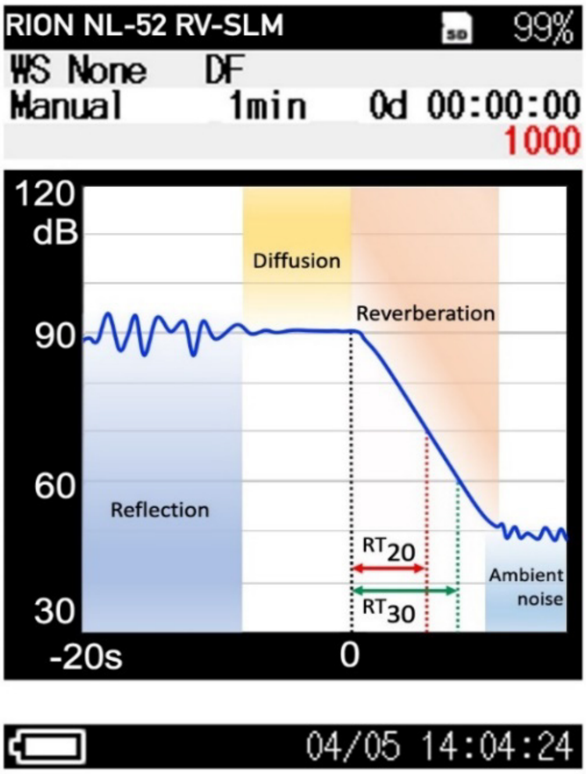

Figure 5. Decay of sound power with time.

The pink noise generator attached to the loudspeaker was switched on, and when the SLM displayed steady sound level of 90 dB (Figure 5), it was switched off. The time lapse to reduce the sound level by 20 and 30 dB were then measured from the decay curve recorded by the SLM. The test was repeated for 5 times to minimise the variation in decay curve. Average RT60 value was calculated from values of RT20 and RT30 (Eq. 2(a), 2(b)). The lower limit of -20 s (Figure 5) signified that necessary time lapsed for the sound level to reach a diffused acoustic field in the hexahedron box before the pink noise generator was switched off.

RT60 (from RT20) = 3 × (time to decay by 20 dB), (2(a)).

RT60 (from RT30) = 2 × (time to decay by 30 dB). (2(b)).

2.7. Determination of Noise Absorption Coefficient Using Impedance Tube

Absorption coefficient of jute felt was measured in the impedance tube (Make-BSWA, China) as per ISO 10534-2: 1998 adopting transfer function method. The circular jute felt sample of φ 30 mm and φ 100 mm were tested against the rigid back wall using two tubes. The larger diameter tube (φ 100 mm) was used to measure the absorption coefficients in the frequency range, 63–1600 Hz, and a smaller diameter tube (φ 30 mm) was used for measuring in the frequency ranges from 1000Hz – 6300 Hz. The jute felt was tested five times to minimize the influence of variation of thickness and areal density.

3. RESULTS AND DISCUSSION

3.1. Diffused Acoustic Field Inside the Hexahedron Box

Each of 7 microphone positions (0.5 to 2.00 m) from loudspeaker along the diagonal length of the reverberation box, were used to measure the sound power to verify the DAF condition. The Figure 6 shows 'A-weighted' sound power (dB)[23] along diagonal length of the hexahedron box measured by SLM after 30s of excitation of pink noise generator. The marginal difference of sound power at 7 positions established the DAF condition inside the hexahedron box. The acoustic field of the box was set with lower and higher boundary of 250 and 6300 Hz respectively. The threshold 250 Hz (higher than Schroeder frequency [24]) caused generation of ray energy condition while highest frequency 6300 Hz confirmed the absence of air attenuation [25]. Moreover, the use of rigid glass fiber composite based smooth wall of box reduced the reflection losses. So, the reverberation time of the fabricated box was long, and the sound effect took more time to die out. The noise absorption coefficient of the box was 0.02 when tested without any felts installed. This value was used to correct the measured noise absorption coefficient of the samples.

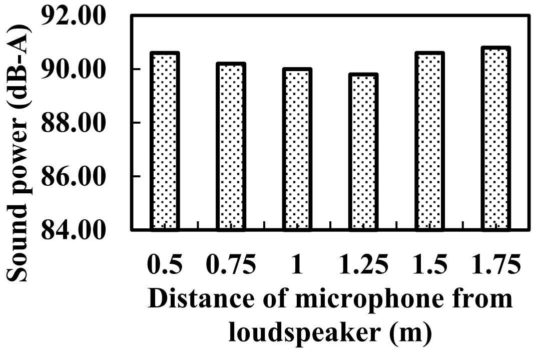

Figure 6. A-weighted sound power (dB) along diagonal length of the hexahedron box.

3.2. Effect of Type of Fibrous Porous Absorber Evaluated in Impedance Tube

The ten different fibrous felts, with an average thickness of 15 mm, and of 1650 g/m^2 areal density were tested in an impendence tube at a central frequency of 1/3rd octave band.

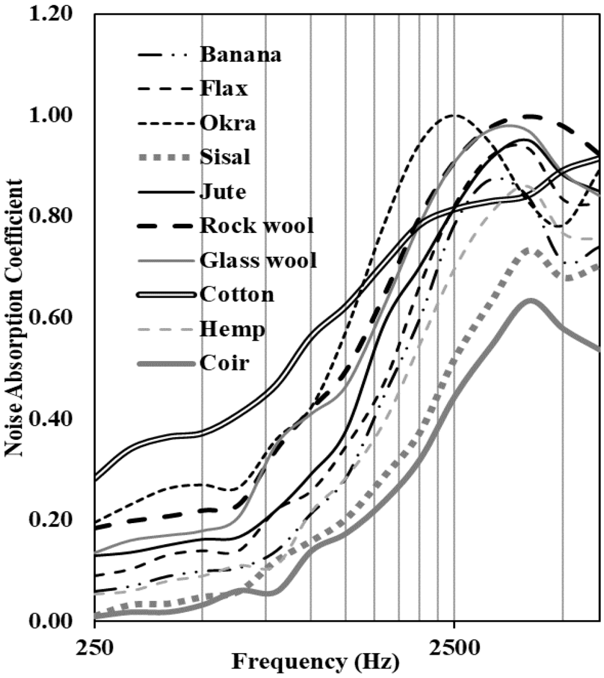

Figure 7. Noise absorption vs frequency curves of 10 different fiber felts (impedance tube).

Figure (7) shows that below 1600 Hz, the fibrous felts were ineffective at controlling the gigantic sound energy. At a frequency of 1600 Hz, the noise absorption coefficients (NAC) of cotton and okra fiber felts were estimated 0.71 and 0.79, whereas sisal and coir felts had NAC values of 0.29 and 0.24 respectively. The NAC was about 0.39 for the other natural fiber-based felts, such as hemp, flax, and banana. Above 1600 Hz, it was observed that noise control performance of jute felt (NAC, 0.55) was on par with that of the commercially available man-made fibers felts (rockwool and glasswool). The results make it more likely that the study will continue with jute felt.

3.3. Effect of Type of Fibrous Porous Absorber Evaluated in Reverberation Box

The study of reverberation time in hexahedron box for 10 fibrous felt revealed that the time gap to reduce the sound power by 60 dB after cessation of pink noise generator reduced with the increase in frequency of sound energy. The DAF inside the hexahedron box prevailed the condition like box with little or no absorption especially at low frequency (250 Hz), which related with higher magnitude of RT60. With the increase in frequency, the fibrous felt became more effective in reduction of sound power caused the lowering RT60 value (Figure 8). The lowest RT60 was found in case of cotton followed by okra felt while the sisal and coir did not show any encouraging result which can be corroborated by NAC study by transfer matrix method (TMM). The performance of jute felt was much comparable to glass and rockwool.

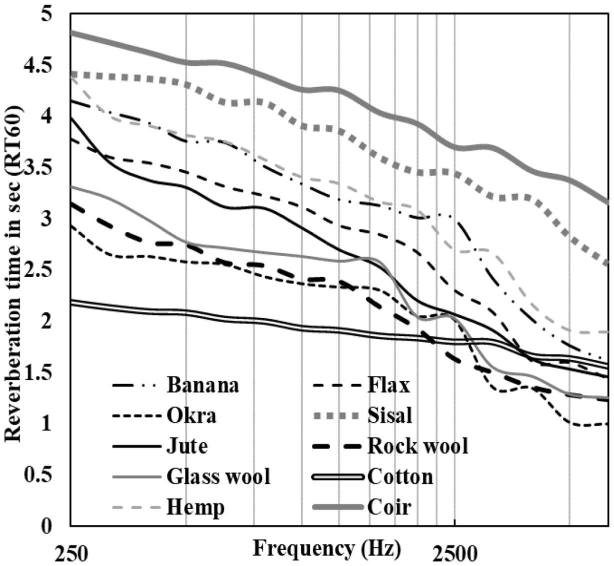

Figure 8. Reverberation time vs frequency curves of 10 different fiber felts (hexahedron reverberation box).

It is to be noted that the jute felts of 15 mm showed much similar trend in noise control behavior (NAC, RT60) to other commercially available manmade fiber felt of 40 mm. So, further study to understand the effect of thickness in TMM and as well DAF conditions was carried out with widely available jute fiber based felts. The polygonal multicellular cross section of the jute fiber with ridges on the surface (Figure 9) of the fiber offers the resistance to propagation of air, the carrier of sound may be responsible for likewise noise control behavior of glass and rockwool fiber.

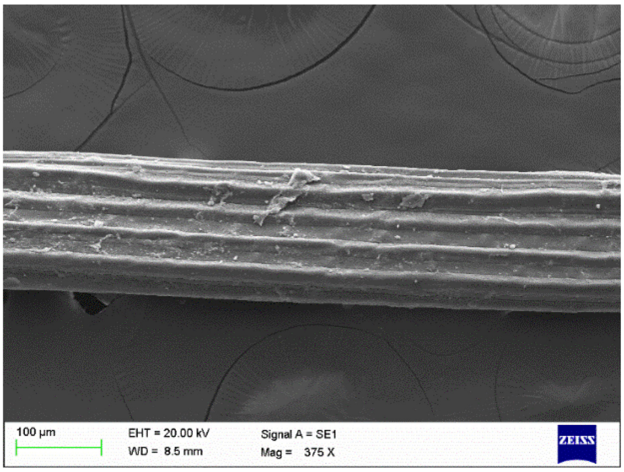

Figure 9. Scanning electron micrograph of jute fiber surface.

3.4. Effect of Thickness of Jute Felt: Impedance Tube

The jute felt was stacked layer after layer (up to 7 layers) and tested in impedance tube at over 15 different frequencies (250 to 6300 Hz of 1/3 octave band). Figure (10) shows that the prominent peak of the sound absorption coefficient moved to the low-frequency range for jute felts with increased number of layer (1 to 7). The attainment of absorption of 90% sound energy at lower frequency is more prominent at higher thickness. The noise absorption coefficients for jute felt at different frequencies increase with its thickness. Jute felt with 37 mm thickness offers absorption of 0.9 at 970 Hz as shown in Figure 10.

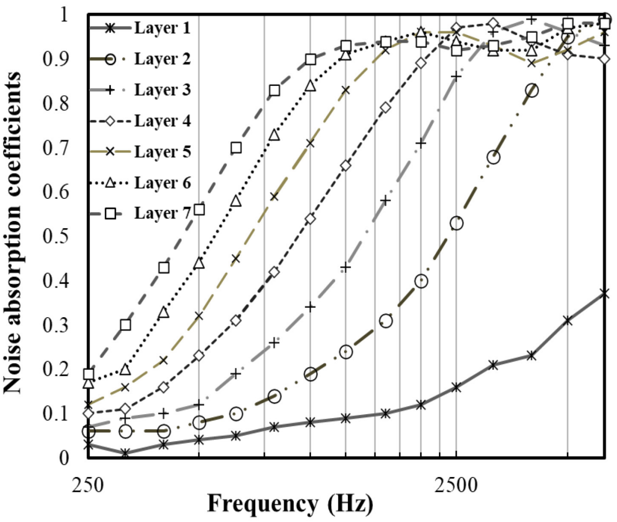

Figure 10. Noise absorption coefficient up to 7 layers of jute felt measured in impedance tube.

The noise control performance of a porous absorber was influenced by its thickness and the way the sample was mounted in the instrument [26]. The variation in thickness of jute felt in impedance tube and the corresponding NAC results over 15 frequencies indicate that jute felt with higher thickness was more efficient to absorb sound energy at low frequency. With the increasing thickness of the porous body, the enhanced length of pore channels caused more loss of energy. The result corroborated the observation of Seddeq [27].

There lies a relationship between thickness and frequency which can be written as follows,

$$f_s \times t = \text{constant}$$

where, f_s being the starting frequency with a sound wave absorption coefficient > 0.6 and 't' is the thickness of the porous body. Thus, the relation explains the law of rectangular hyperbola with x- and y-axis, as asymptotes. Figure (11a) shows that for a given value of thickness, the increment of absorption from 0.7 to 0.9 was related to a higher magnitude of frequency viz., 3196 to 4688 Hz with lower wavelength (λ) of sound energy. The two-layer stack of jute felt with an average thickness of 10.1 mm offered 90% absorption of sound energy at a frequency of 4688 Hz. While the seven-layer stack of jute felt (thickness, 37mm) offered an increase of absorption from 70% to 90% by tackling a frequency of 970 Hz other than 626 Hz with higher λ as shown in Figure 11 a. The figure (Figure 11 a) shows that the relation of frequency and thickness of jute felt is a rectangular hyperbola, which would be expressed in a generic form as follows.

$$f_s \times t^m = b \tag{3}$$

where, m being the power term of thickness, and b is constant as presented in Figure 11b. The error bars are shown in graph (Figure 11 b) represent that the variability of 'm' and 'b', which were found to be statistically insignificant at a 5% confidence level. Equation (3) may be used to determine the thickness of jute felt to deal with a given frequency for noise absorption above 70% (NAC, 0.7).

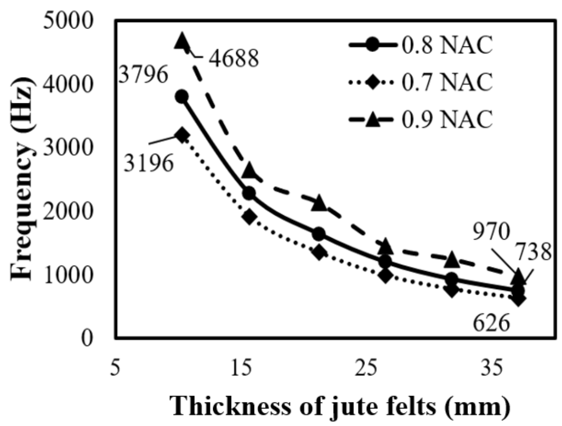

Figure 11 a. The plot of frequency (Hz) as a function of thickness absorption coefficients of 0.7, 0.8 and 0.9.

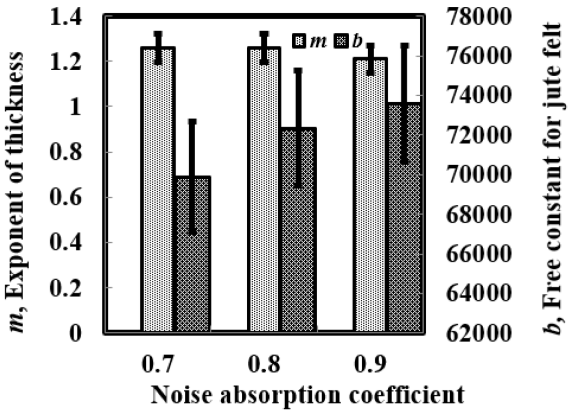

Figure 11 b. Exponent of thickness, 'm' and constant, 'b' at 70, 80, and 90% noise absorption of jute felt.

3.5. Effect Of Thickness of Jute Felt: Reverberation Box

It was observed that the RT60 at threshold frequency of 250 Hz varied from 3.6 s (seven layer, jute felt) to 2.8 s (one layer jute felt). The thickness of one layer jute felt was too small to the wavelength at lower frequency (250 Hz). Thus, the felt was ineffective to absorb the complex sound of low frequency, while at higher frequency the fibrous jute felt of a given thickness absorbed more amount of energy from the sound wave as it passes through the felt. Thereby sound energy with higher frequency, can be controlled effectively by the jute felt. Figure (12) depicts that the reverberation time (RT60) decreased with the thickness of the jute felts, which can be supported by the noise control behavior jute felt test under TMM condition. The higher thickness of the fibrous material, associated with more absorption of sound energy, thus reduced the time lapse to cut down the sound power by 60 dB.

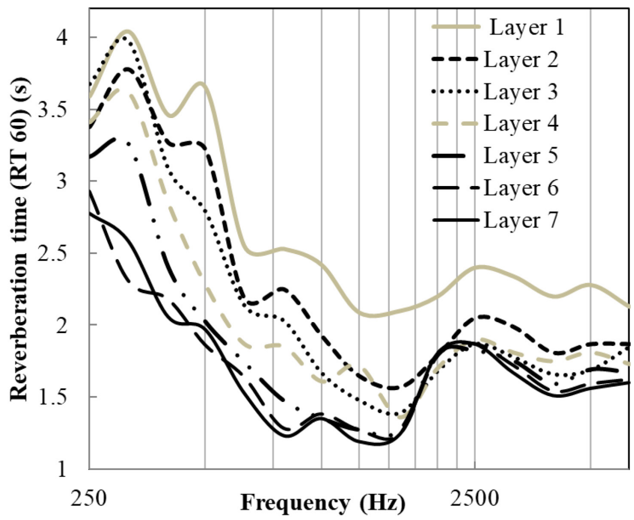

Figure 12. Reverberation time up to 7 layers of jute felt measured in hexahedron reverberation box.

3.6. Development of Frequency Dependent New Model of Absorption from Reverberation Time

The noise control studies (TMM and DAF condition) of the fibrous absorbers (felts) revealed that their performance was very much frequency dependent. Apparently, an absorber with higher noise control property at high frequency could not perform effectively to control noise at lower frequency. Since propagation of sound energy through fiber felt is a complex phenomenon, the NAC value of the same sample changes with frequency. Thereby, frequency was identified as an important factor to deal with, during the study of noise control.

The impedance tube data computed to predict NAC as a function of RT60 and frequency, eliminated the influence of thickness of the fiber felts. The noise absorption coefficient was dependent on the frequency and the value of NAC increased with an increase in the magnitude of frequency i.e., with a decrease in wavelength of sound energy (Figure 10 and Figure 11a). It was observed that the nature of RT curves inside the reverberation box changes with frequency (Figure 8, 12) due to transition from individual resonances to overlapped normal modes. Besides, the reverberation box was designed with a minimum distance between the opposite walls greater than the half of maximum wavelength to deal with frequency as low as 250 Hz. So, a frequency dependent model was needed to establish, where frequency and reverberation time (RT60) were the independent variables and noise absorption coefficient was the dependent one. A three dimensional (3D) plotting of noise absorption coefficient as a function of RT60 and frequency is presented in Figure 13.

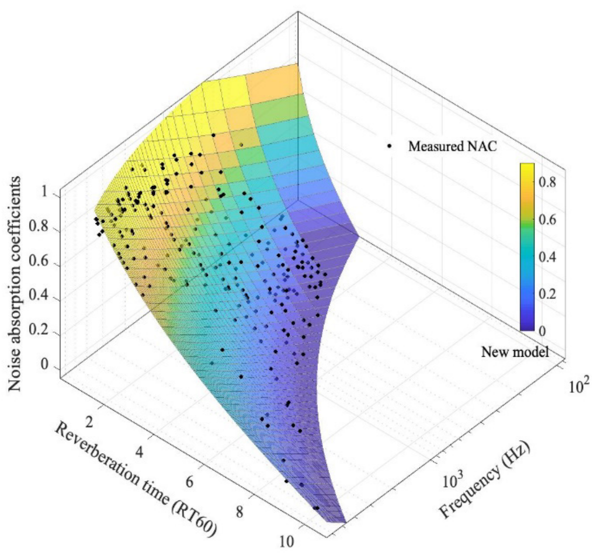

Figure 13. Frequency dependent new model of estimation of noise absorption coefficients.

The prediction surface model (Eq. 4) explained that the NAC increases with frequency and decreases with RT60. The developed model has now been effective to predict the noise absorption coefficient, and the frequency dependent new model can be written as follows.

$$a_{newmodel} = f^{p} + \frac{q}{RT\,60^{\,r}} \qquad (4)$$

where, $p = 0.1024$, $q = -1.228$ and $r = -0.2854$, and f in Hz as estimated from the response surface equation.

3.7. Validation

Verification of frequency dependent new model (Equation 4) was carried out for three samples of particle board based perforated absorber, as shown in Figure 4. Experimental results of 3 samples in TMM condition (continuous lines in Figure 14) were plotted along with the predicted NAC from RT60 measured in DAF condition (solid dots, Figure 14, Equation 4).

The measured plots of three samples in TMM condition agreed fairly well with new model based prediction. The calculated NAC at 15 central frequencies of 1/3rd octave band followed the profiles of the measured graphs with a mean absolute error as low as 0.02.

4. CONCLUSION

The report recited over the data generated through the designed nonregular hexahedron reverberation box with non parallel opposite walls reflected and diffused the sound power in all possible directions and created the ‘diffused acoustic field’ condition for a frequency range of 250 to 6300 Hz. The acoustic field of the box with its lower and higher frequency caused generation of ray energy condition and confirmed the absence of air attenuation. Moreover, the use of rigid glass fiber composite based smooth walls of the box, reduced the reflection losses. So, the reverberation time of the fabricated box was long, and the sound power took more time to die out.

The noise control studies (TMM and DAF conditions) revealed that an absorber with higher noise control properties at high frequency could not perform effectively to control noise at lower frequency. Thereby, frequency was identified as an important factor to deal with, during the study of noise control. The NAC calculated from RT60 measured in hexahedron reverberation box synchronized with impedance tube results and an empirical model was formulated and validated with particle board based perforated absorber with mean absolute error about 0.02.

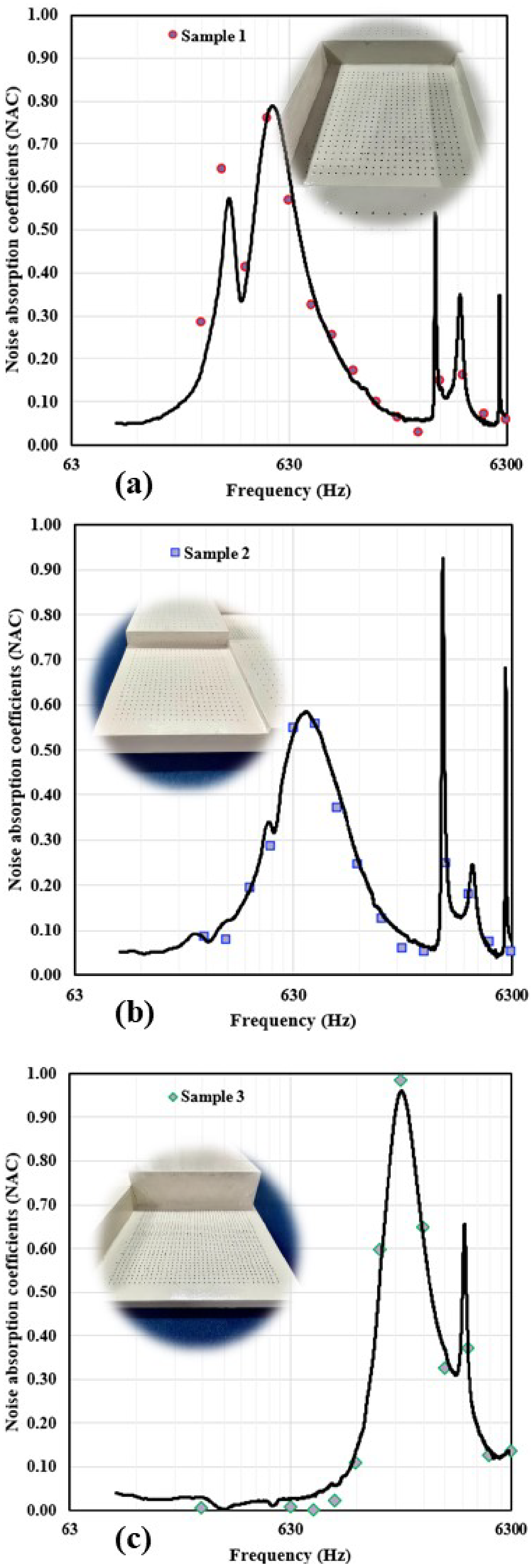

Figure 14 New model correlation with measured NAC.

The design of the reverberation box eased the evaluation of the acoustic performance of a sample with a smaller size and thus eliminated the need of large test samples which are being used in presently available reverberation rooms. In addition, the developed box provided a nondestructive mode of testing. The fabricated reverberation box supported by castors paddle brakes with enhanced portability, and simplicity in sample mounting process through collapsible aperture has made it user friendly.

ACKNOWLEDGMENTS

This work was supported by ICAR-National Agricultural Science Fund, New Delhi, India [grant number NASF/ME/5016/2015-16].

REFERENCES

[1] A. T. de Hoop and J. G. Harris, “Handbook of radiation and scattering of waves: Acoustic waves in fluids, elastic waves in solids, electromagnetic waves,” *J. Acoust. Soc. Am.*, vol. 109, no. 5, pp. 1763–1763, May 2001, doi: 10.1121/1.1356700.

[2] C. Foreman, “Sound system design,” in *Handbook for sound engineers*, 4th ed., G. M. Ballou, Ed. Amsterdam; Boston: Focal Press, 2008, pp. 1233–1335.

[3] Y. Na, J. Lancaster, J. Casali, and G. Cho, “Sound absorption coefficients of micro-fiber fabrics by reverberation room method,” *Text. Res. J.*, vol. 77, no. 5, pp. 330–335, May 2007, doi: 10.1177/0040517507078743.

[4] G. Petrone, V. D’Alessandro, F. Franco, and S. De Rosa, “Damping evaluation on eco-friendly sandwich panels through reverberation time (RT60) measurements,” *J. Vib. Control*, vol. 21, no. 16, pp. 3328–3338, Dec. 2015, doi: 10.1177/1077546314522507.

[5] S. R. Bistafa and J. S. Bradley, “Reverberation time and maximum background-noise level for classrooms from a comparative study of speech intelligibility metrics,” *J. Acoust. Soc. Am.*, vol. 107, no. 2, pp. 861–875, Feb. 2000, doi: 10.1121/1.428268.

[6] J. Cucharero, T. Hänninen, and T. Lokki, “Influence of Sound-Absorbing Material Placement on Room Acoustical Parameters,” *Acoustics*, vol. 1, no. 3, pp. 644–660, Aug. 2019, doi: 10.3390/acoustics1030038.

[7] D. Vigé, “Vehicle interior noise refinement – cabin sound package design and development,” in *Vehicle Noise and Vibration Refinement*, Elsevier, 2010, pp. 286–317. doi: 10.1533/9781845698041.3.286.

[8] A. Nash, “On the reproducibility of measuring random incidence sound absorption,” *J. Acoust. Soc. Am.*, vol. 130, no. 4, pp. 2354–2354, Oct. 2011, doi: 10.1121/1.3654430.

[9] M. Hodgson, “When is diffuse-field theory applicable?,” *Appl. Acoust.*, vol. 49, no. 3, pp. 197–207, Nov. 1996, doi: 10.1016/S0003-682X(96)00010-2.

[10] A. Abdou and R. Guy, “A review of objective descriptors for sound diffuseness,” *Can. Acoust. Internet*, vol. 22, no. 3, pp. 43–44, 1994, [Online]. Available: https://jcaa.caa-aca.ca/index.php/jcaa/article/view/841

[11] N. Epain and C. T. Jin, “Spherical Harmonic Signal Covariance and Sound Field Diffuseness,” *IEEEACM Trans. Audio Speech Lang. Process.*, vol. 24, no. 10, pp. 1796–1807, Oct. 2016, doi: 10.1109/TASLP.2016.2585862.

[12] C.-H. Jeong, M. Nolan, and J. Balint, “Difficulties in comparing diffuse sound field measures and data/code sharing for future collaboration,” presented at the Conference: Proceedings of Euronoise 2018, Heraklion, Crete, May 2018. doi: 2018.

[13] O. Robin, A. Berry, O. Doutres, and N. Atalla, "Measurement of the absorption coefficient of sound absorbing materials under a synthesized diffuse acoustic field," *J. Acoust. Soc. Am.*, vol. 136, no. 1, pp. EL13–EL19, Jul. 2014, doi: 10.1121/1.4881321.

[14] X. Zhou, M. Späh, K. Hengst, and T. Zhang, "Predicting the reverberation time in rectangular rooms with non-uniform absorption distribution," *Appl. Acoust.*, vol. 171, p. 107539, Jan. 2021, doi: 10.1016/j.apacoust.2020.107539.

[15] R. O. Neubauer, "Estimation of reverberation time in rectangular rooms with non-uniformly distributed absorption using a modified fitzroy equation," *Build. Acoust.*, vol. 8, no. 2, pp. 115–137, Jun. 2001, doi: 10.1260/1351010011501786.

[16] T. Khajah, X. Antoine, and S. P. A. Bordas, "B-Spline FEM for Time-Harmonic Acoustic Scattering and Propagation," *J. Theor. Comput. Acoust.*, vol. 27, no. 03, p. 1850059, Sep. 2019, doi: 10.1142/S2591728518500597.

[17] F. Fahy, "Sound in enclosures," in *Foundations of Engineering Acoustics*, Elsevier, 2001, pp. 236–269. doi: 10.1016/B978-012247665-5/50010-2.

[18] E. J. Carlisle and R. J. Hooker, "Small Chamber Reverberant Absorption Measurement," in *Proceedings of ACOUSTICS 2004*, Gold Coast, Australia, 2004, pp. 89–92. [Online]. Available: https://acoustics.asn.au/conference_proceedings/AAS2004/ACOUSTIC/PDF/AUTHOR/AC040072.PDF

[19] M. Long, "Vibration and vibration isolation," in *Architectural acoustics*, Second edition., Boston: Academic Press, 2014, pp. 417–455.

[20] P. S. Liu and G. F. Chen, "Characterization Methods," in *Porous Materials*, Elsevier, 2014, pp. 493–532. doi: 10.1016/B978-0-12-407788-1.00010-1.

[21] C. Foreman, "Sound system design," in *Handbook for Sound Engineers*, 4th ed., G. M. Ballou, Ed. Burlington: Focal, 2005, pp. 1233–1335. [Online]. Available: https://www.pdfdrive.com/handbook-for-sound-engineers-d163076376.html

[22] K. Mostafa and P. Shalkouhi, "The Schroeder frequency of furnished and unfurnished spaces.," *Romanian J. Acoust. Vib.*, vol. 9, no. 2, pp. 113–116, 2012.

[23] T. Fujiwara, S. Meiarashi, Y. Namikawa, and M. Hasebe, "Reduction of equivalent continuous A-weighted sound pressure levels by porous elastic road surfaces," *Appl. Acoust.*, vol. 66, no. 7, pp. 766–778, Jul. 2005, doi: 10.1016/j.apacoust.2004.12.004.

[24] M. Meissner, "The discrete Hilbert transform and its application to the analysis of reverberant decay of modal vibrations in enclosures," *J. Vib. Control*, vol. 18, no. 11, pp. 1595–1606, Oct. 2012, doi: 10.1177/1077546311420896.

[25] R. H. C. Wenmaekers, C. C. J. M. Hak, and M. C. J. Hornikx, "The effective air absorption coefficient for predicting reverberation time in full octave bands," *J. Acoust. Soc. Am.*, vol. 136, no. 6, pp. 3063–3071, Dec. 2014, doi: 10.1121/1.4901710.

[26] H. S. Seddeq, "Factors influencing acoustic performance of sound absorptive materials," *Aust. J. Basic Appl. Sci.*, vol. 3, no. 3, pp. 4610–4617, 2009.

[27] H. S. Seddeq, N. M. Aly, A. Marwa A, and M. Elshakankery, "Investigation on sound absorption properties for recycled fibrous materials," *J. Ind. Text.*, vol. 43, no. 1, pp. 56–73, Jul. 2013, doi: 10.1177/1528083712446956.